Chapter 1
Fundamentals of Acoustic Cavitation in Sonochemistry

Jia Luo, Zhen Fang, Richard L. Smith, Jr. and Xinhua Qi

Abstract Acoustic cavitation is the main mechanism for reaction intensification in sonochemistry. This chapter provides an overview of the dynamics, mechanisms and theories of acoustic cavitation. Through mathematical simulation and experimental observation, single bubble cavitation theory describes the radial growth, oscillation and energy behavior of a single bubble in a low frequency acoustic field. In multibubble cavitation, the bubble dynamics and energy are greatly influenced by neighboring bubbles. Many hypotheses, such as rectified diffusion, bubble coalescence, concerted collapse and bubble cloud theory, and experiment methods, are used to describe multibubble behavior and energy intensity. Factors such as liquid properties, acoustic field parameters and heterogeneous characteristics of reaction system influence acoustic cavitation. Adverse effects from heterogeneous characteristics on acoustic cavitation can be analyzed to improve the efficiency of sonochemical reactors. The introduction of sonication into a chemical system allows intensification of many reactions, however, proper design of acoustic equipment is needed to obtain reliable results.

Keywords Ultrasonic auxiliary · Acoustic cavitation · Bubble dynamics · Heterogeneous chemical system

J. Luo · Z. Fang (✉)
Biomass Group, Key Laboratory of Tropical Plant Resources and Sustainable Use, Xishuangbanna Tropical Botanical Garden, Chinese Academy of Sciences, Kunming, China
e-mail: zhenfang@xtbg.ac.cn

R.L. Smith, Jr.
Research Center of Supercritical Fluid Technology, Tohoku University, Sendai, Japan

X. Qi
College of Environmental Science and Engineering, Nankai University, Tianjin, China

Z. Fang et al. (eds.), *Production of Biofuels and Chemicals with Ultrasound*, Biofuels and Biorefineries 4, DOI 10.1007/978-94-017-9624-8_1

1.1 Ultrasound and Acoustic Cavitation

Ultrasound is a longitudinal pressure wave that has a wave frequency higher than normal human hearing range. In acoustic science, the classification of a sound wave is according to its oscillating frequency. Waves that have oscillating frequencies from 0.001 to 10 Hz are referred to as infrasonic sound, and waves with oscillating frequencies from 16 kHz and higher are referred to as ultrasonic sound or ultrasound [1]. Table 1.1 lists some key parameters including the wavelength, speed, frequency, amplitude, power, pressure, intensity of acoustic wave, acoustic characteristic impedance of medium material and their typical values in sonochemistry [1].

Compared with audible sound and other wave phenomena, ultrasound causes many special physical or chemical effects in materials. Because of the high oscillating frequency of liquid molecules in an ultrasonic field and the high viscosity of the liquid medium compared with a gas, molecules absorb a large number of energy from the propagating ultrasonic wave. As shown in Table 1.1 for the acoustic pressure, liquid reactants in ultrasonic field can have a high pressure difference relative to the hydrostatic pressure of fluid [2]. The high energy absorption and high acoustic pressure make it possible for ultrasonic auxiliary to overcome intermolecular interactions in a solvent, and produce numerous cavities, which is referred to as acoustic cavitation. The formed cavities drain and accumulate ultrasonic energy, and explosively release their energy by the collapse of cavities. Therefore, there are two main routes that ultrasound provides energy to liquid reactants: (i) ultrasonic microstreaming (mechanical force) and (ii) acoustic cavitation. However, only acoustic cavitation is believed to activate chemical reactions with high energy intensity.

As shown in Table 1.1, ultrasound is used in power applications at low frequencies of 20–40 kHz and at high acoustic power (>50 W), or it can be used in nondestructive detection or measurement at frequencies above 1 MHz and low acoustic power as commonly used in diagnostics, clinical medicine and biological processing.

In this chapter, the fundamentals in ultrasound and acoustic cavitation are introduced. The dynamics and influencing factors of cavitation bubbles are summarized. The secondary effects of acoustic cavitation are introduced and discussed. The knowledge may be useful in studying the intensification mechanism of sonochemical reaction of biomass materials. The authors would like to emphasize the relationship between energy intensity and energy efficiency with sonication. The ability of cavitating bubbles to focus and concentrate energy, forces and stresses is the basic of phenomena for ultrasonic auxiliary of biomass-related reactions [3], while the development of bioenergy requires attentions to special energy intensity that could activate chemical species and possibly lower energy cost.

Table 1.1 Key parameters in acoustic science and typical parameter values for studies in sonochemistry [1]

Parameters (*symbol*, unit)	Physical definition	Typical values
Acoustic wavelength (λ, m)	Distance between two neighboring points that have the same phase position in an acoustic wave	3.0–7.5 cm for power ultrasound in liquids
		0.015–0.075 cm for measurement
Acoustic speed (c, m/s)	Acoustic propagation distance per unit time	Air, 340 m/s
		Liquid, 1,000–2,000 m/s
		Solids, 3,000–6,000 m/s
Acoustic frequency (f, Hz)	Vibration number per unit time	20–40 kHz for power ultrasound in liquids
		1–20 MHz for measurement
Acoustic amplitude (P_A, m)	Maximum distance of mass point at the ultrasonic field from its balance position	
Acoustic power (P, W)	Acoustic energy that passes through one surface perpendicular to the propagating direction per unit time	Extremely high power (>1,000 W) for cavitational erosion of solids and metal working
	Optimum acoustic power depends on sample, reactor volume and processing needs	High power (50–1,000 W) for ultrasound-assisted conventional thermochemical and biochemical reactions
		Low power (1–10 W) for stimulating biological cells or for promoting particle aggregation with low cavitation
Acoustic pressure (P_a, Pa)	Difference of dynamic force per area from its static value, as the result of the compressed zone and rarefacted zone of fluid formed with sound transport	0.1–1 MPa for ultrasonic cleaner
	$P_a = P_A \sin(2\pi ft)$, where t refers to the propagating time	
Acoustic intensity (I, W/m^2)	Average acoustic energy that passes through a unit surface perpendicular to the propagating direction per unit time	
	Vector $I = P_A^2/(2\rho c)$, where ρ is the medium density	
Acoustic characteristic impedance (Z, kg/(m^2 s))	Ratio of acoustic pressure to acoustic velocity at one mass point in the medium	Gases, 1.1–5.5 $\times$ 10^2 kg/(m^2 s)
		Liquids, 0.7–3.2 $\times$ 10^6 kg/(m^2 s)
		Nonmetals, 0.1–1.5 $\times$ 10^7 kg/(m^2 s)
	Characteristic of the transmitting medium. $Z = \rho c$, where ρ is the medium density	Metals, 1.0–10.4 $\times$ 10^7 kg/(m^2 s)

1.2 Acoustic Cavitation

The energy content of ultrasonic microstreaming is relatively low due to the small amplitude of the oscillation of fluid elements and it is generally insufficient to induce chemical reaction in the medium. The wavenumber of ultrasound in liquid is much larger than ultraviolet light, and the excitation of electrons in compound molecules is not possible with sonication. Sonication does not result in the resonance of chemical molecules or atoms like other methods such as microwave or infrared radiation, because the oscillating frequency of ultrasound is on the order of 10^4–10^5 Hz. As a result, acoustic cavitation, which could concentrate and explosively release acoustic energy, is believed to be the dominant mechanism for process intensification and chemical activation in sonochemical systems.

1.2.1 Dynamics and Energy of Single Bubble Cavitation

The complete process of acoustic cavitation consists of three steps [4, 5]:

1. Formation of cavitation nuclei. Figure 1.1 shows bubble formation, growth and collapse phenomena for transient and steady cavitation. Negative and positive acoustic pressure act alternately on one point in the liquid medium in an ultrasonic cycle with the propagation of ultrasound wave (Fig. 1.1). The negative acoustic pressure stretches the liquid medium apart to make a relatively rarefacted zone. If the acoustic pressure is increased to a value that is higher than certain intensity, the microscopic distance between the liquid molecules becomes far enough to initiate cavity formation that contains solvent vapors or dissolved gases. The minimum requirement for acoustic pressure to form a cavity is called the Blake threshold, P_B. If the vapor pressure in a bubble can be ignored, then Eq. 1.1 results [5]:

$$P_B = P_0 + \frac{2}{3}\left[\frac{(2\sigma/R_0)^3}{3(P_0 + 2\sigma/R_0)}\right]^{1/2} \tag{1.1}$$

where P_0 is the static pressure on the liquid, R_0 is the initial radius of the formed bubble, and $2\sigma/R_0$ is the surface tension of the assumed bubble when it forms. Low surface tension and low static pressure on a liquid favors the formation and growth of cavitation nuclei. The existence of impurities and heterogeneous crevices in liquids decrease the actual pressure threshold of cavitation by reducing the surface tension. The Blake threshold value for untreated solvents is about 1–10 % of that in ultrapure solvents [4]. The influence of impurities and heterogeneous crevices on nucleation is kinetic. Similarly to a catalyst, the presence of surface defects lowers the free energy barriers separating the metastable liquid state from the vapor phase, and modifies the nucleation

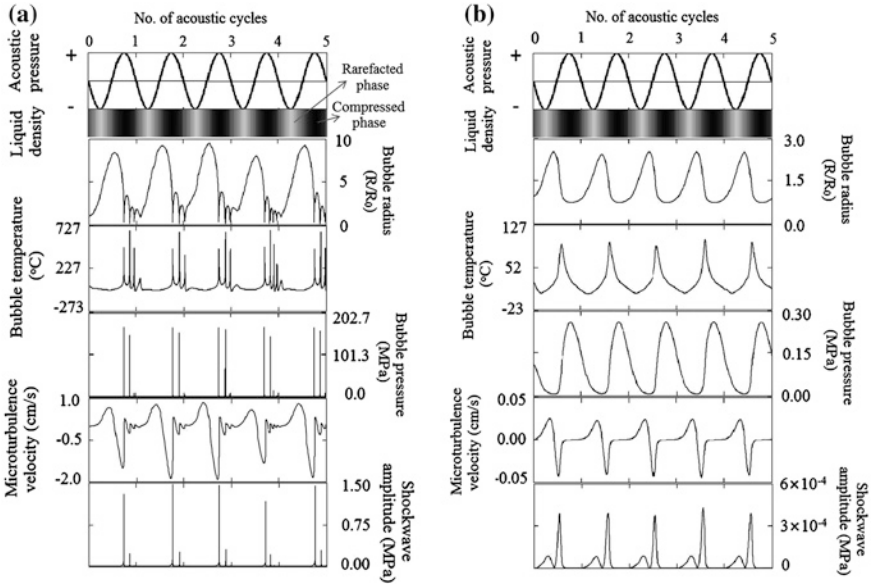

Fig. 1.1 Calculation results of bubble dynamics: **a** transient cavitation and **b** steady cavitation: acoustic pressure, bubble temperature, microturbulence velocity, bubble radius, bubble pressure, and shockwave amplitude (adapted with permission from [8], Copyright © 2012 Elsevier)

mechanism [6]. As a result, the nucleation rate on surface defects with simple geometries can be increased by up to five orders of magnitude compared with that of a flat hydrophobic surface [6]. The presence of surface defects has also been found to affect the nucleation rate for non-condensable gas as dissolved in liquids [6]. For bubble nucleation in solutions containing solid substances, the contact angle of gas bubbles on the solid surface is a critical index to evaluate the possibility of bubble nucleation. A small contact angle means a low energy barrier for the nucleation. In recent research by Zhang et al. [7], it was pointed out that the contact angle of gas bubbles on spherical surfaces could be remarkably reduced by several methods such as decreasing the surface tension of the solution, by reducing the size of solid particles, or by changing the hydrophilic surface of solid particles to that of a hydrophobic surface.

2. Growth (radial motion) of cavitation bubbles. The formed microbubble continually grows to a maximum bubble radius of about 2–150 μm until the end of the negative acoustic pressure phase. The oscillating motion of cavitation bubble can be described with the Rayleigh-Plesset equation [5]:

$$R\frac{d^2R}{dt^2}+\frac{3}{2}\left(\frac{dR}{dt}\right)^2=\frac{1}{\rho}\left[\left(P_0+\frac{2\sigma}{R_0}\right)\left(\frac{R_0}{R}\right)^{3\gamma}-\frac{2\sigma}{R}-\frac{4\mu}{R}\left(\frac{dR}{dt}\right)-P_\infty\right] \quad (1.2)$$

where R is the radius of bubble in motion, dR/dt is the velocity item of bubble wall away from the bubble center, R_0 is the initial radius of bubble, ρ and μ are the density and viscosity of the liquid, γ refers to the specific heat ratio of gas in bubble and the P_0 and P_∞ are the static pressure nearby bubble and at infinite distance in the liquid. The terms on the left-hand side of the equation represent the radial motion (expansion or compression) of the bubble wall. On the right-hand side of the equation, the first term shows the pressure variation in the bubble, while the second and third terms are the surface tension and the viscous stresses at the bubble surface, respectively. Equation 1.2 is based on the assumption that the motion of a bubble is adiabatic and that the liquid is incompressible [4]. The mass and heat transfer between the bubble and the surroundings is not considered in Eq. 1.2. It is assumed that no chemical reaction or physical changes occur and that there are no temperature, density or pressure gradients in cavitating bubble.

3. Collapse or the next oscillation of bubbles. Positive acoustic pressure phase comes after the negative pressure phase (Fig. 1.1), and under its influence, the cavitation bubble undergoes contraction. The time required for the bubble to contract is about 25–0.5 μs, which is half of the reciprocal of ultrasound frequency. According to the literature [9], the oscillating frequency of a bubble in a liquid, f_b, increases with contraction of the bubble radius, R:

$$f_b = \frac{1}{2\pi R}\left[\frac{3\gamma}{\rho}\left(P_0 + \frac{2\sigma}{R}\right)\right]^{1/2} \tag{1.3}$$

where ρ is liquid density, γ and $2\sigma/R$ are the gas specific heat ratio and surface tension in the bubble and P_0 is the static pressure. If the resonant frequency of a bubble, f_b, is smaller than the frequency of ultrasonic field, f_a, at the end of the positive acoustic pressure phase, the bubble survives and turns to growth in a new ultrasonic cycle. The radial motion of the cavitation bubble can be repeated for several acoustic cycles, and is called as steady cavitation (Fig. 1.1b). However, if $f_b \geq f_a$, the bubbles will collapse quickly in several nanoseconds, and this is called as transient cavitation (Fig. 1.1a). Fragments generated during the collapse of the parent bubble may become new nuclei for subsequent cavitation phenomena. Steady and transient cavitation are both present in most sonochemical systems, although the properties of the liquid may favor one type of cavitation.

During the transient collapse of a bubble, work is done by the liquid such that fluid elements impart energy to the bubble, thus raising its temperature and pressure. The energy intensity of the cavitation bubble collapse is proportional to the compression ratio of the bubble at the point of minimum radius during radial motion. At the instance of bubble collapse, energy is released that does not have time to be transferred to the surroundings and therefore local hotspots are produced [10, 11]. These local hotspots have extremely high temperatures (ca. 5,000 °C) and

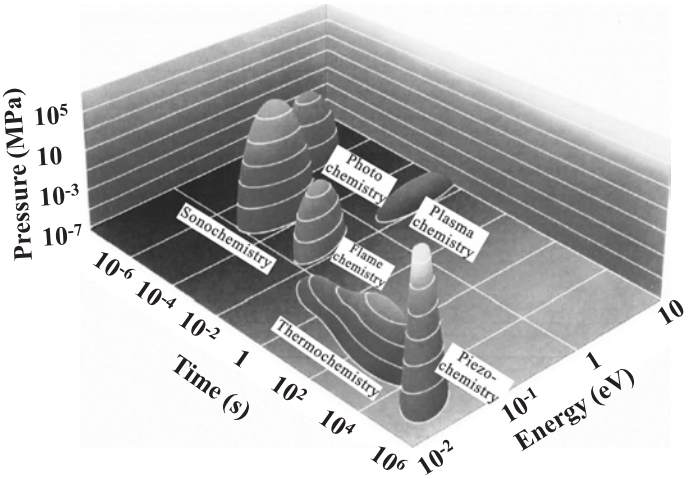

Fig. 1.2 Range of duration time, pressure and energy for various energy chemistries (reprinted with permission from [11], Copyright © 2010 WILEY-VCH Verlag GmbH & Co. KGaA, Weinheim)

pressures (ca. 100 MPa) in its interior, and causes very high rates of local heating and cooling (>10^9 °C/s). The energy density of acoustic cavitation can be on the order of 10^{15} W/cm^3, while the rated acoustic power density used in common sonochemical reactors is 10^{-2}–10 W/cm^3 [12]. Acoustic cavitation also produces high intensity shockwave and violent flowing of localized liquid.

In Fig. 1.2, the average energy of acoustic cavitation (about 0.1–1 eV) is much higher than that in conventional heating, so that breaking most of chemical bonds is possible. However, this energy is not enough for plasma ionization of volatile molecules and photon production in bubbles. Suslick et al. [13, 14] observed very strong Ar atomic excitation in the sonication of 95 wt% sulfuric acid solution at 20 kHz at ambient temperature under an Ar atmosphere. The emission temperature of Ar excitation in bubble was estimated at about 8,000 °C. However, the thermal excitation of Ar atom needed very high energy of >13 eV, and thus Ar atom could not be thermally excited at 8,000 °C, which shows that the distribution of temperature and pressure in a bubble is not uniform. Figure 1.3 shows the physical structure of a bubble and the active zones for sonochemistry. Optically opaque plasma probably exists at the core of a collapsing bubble at extreme conditions, and the collision of higher energy electrons in this plasma zone is believed to result in the excitation of an Ar atom. Spectral lines of Ar excitation are emitted just on the outer zone of the plasma ionization (emissive shell) and can be detected by ultraviolet-visible spectroscopy [14]. The emissive shell is optically transparent and has a temperature that is much lower than the plasma zone.

On the other hand, the energy intensity of bubbles is also influenced by the mass and heat transfer of the surrounding liquid. It is believed that the vapor or gas

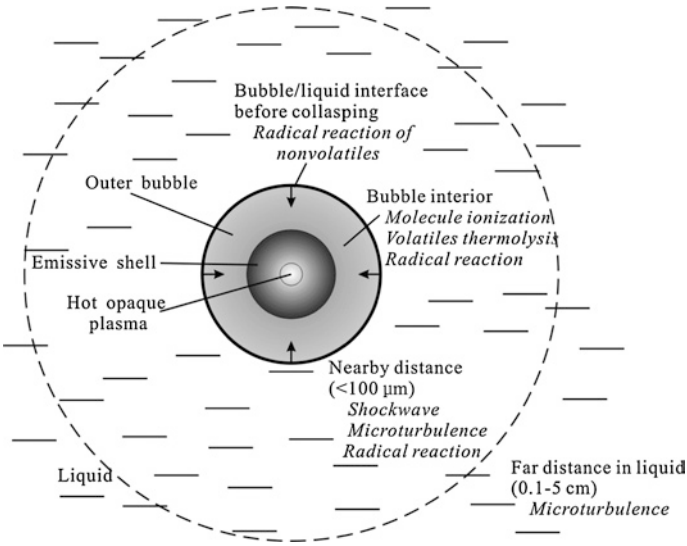

Fig. 1.3 Physical structure of collapsing bubble and active zones for sonochemistry (adapted with permission from [14], Copyright © 2011 Elsevier)

in the cavity can not escape into the surroundings before bubble collapse occurs. However, the evaporation of liquid molecules at the interface between bubbles and surroundings is possible and materials flowing into the bubbles can change the vapor composition in a bubble. Dissociation and chemical reactions of volatile molecules in the bubble can occur and this will consume the energy of the bubble and reduce its energy release when it collapses. For example, sonication in alcohol solution under Ar atmosphere at the frequencies of 20, 363 and 1,056 kHz gives contradictory results [15]. Much less energy is released in a high frequency acoustic field of 1,056 kHz than at low frequencies, which is determined by the volume change of bubbles when bubbles collapse. However, the calculated temperature of the cavitation bubbles has the following order of high to low according to frequencies of 1,056 > 363 > 20 kHz. It is highly possible that the evaporation of solvent in the acoustic field of 20 kHz is more than that at 1,056 kHz, because of the longer acoustic cycle and larger bubble size during the radial motion of bubbles under sonication at 20 kHz.

Therefore, it is necessary to modify the Rayleigh-Plesset equation (Eq. 1.2), because Eq. 1.2 deals with slow bubble motions, and many of the assumptions on which Eq. 1.2 is based are invalid at the time of rapid collapse of bubbles [16]. Equation 1.2 does not take mass transfer, heat transfer, chemical reactions, non-equilibrium phase changes and non-uniform pressures in the bubble interior into account, so that modeling results have large deviations from their true values. Boundary layer approximation on the basis of physical observations allows simplification of the theory.

For example, considering the compressibility of liquid and the acoustic attenuation, the bubble motion can be described by the Keller-Miksis equation (Eq. 1.4) [17, 18]:

$$\begin{aligned}&(1-\frac{dR/dt}{c})R\frac{d^2R}{dt^2}+\frac{3}{2}(1-\frac{dR/dt}{3c})\left(\frac{dR}{dt}\right)^2\\&=\frac{1}{\rho}\left\{(1+\frac{dR/dt}{c})\left[P_b-(P_{\mathrm{am}}-P_A\sin 2\pi ft)\right]+\frac{R}{c}\frac{dP_b}{dt}-\frac{2\sigma}{R}-\frac{4\mu}{R}\left(\frac{dR}{dt}\right)\right\}\end{aligned} \tag{1.4}$$

where R is the radius of bubble in motion, dR/dt is the velocity item of bubble wall away from the bubble center, ρ is the liquid density, μ is the dynamic viscosity of the liquid ($\mu = \rho\nu$, ν is kinematic viscosity), and the c, f and P_{A} are the speed, frequency and pressure amplitude of the sound wave in liquid, respectively. In Eq. 1.4, $2\sigma/R$ is the surface tension of the bubble according to the liquid temperature, P_{am} is the ambient pressure (1 atm), P_{b} is the pressure inside the bubble, and its time derivative is given by a van der Waals type equation of state as Eq. 1.5 [17, 18]:

$$P_g(t)=\frac{N_{tot}(t)kT_b}{\frac{4\pi}{3}\left[(R(t))^3-\left(\mathrm{R}_{eq}(t)/8.86\right)^3\right]} \tag{1.5}$$

In Eq. 1.5, k is the Boltzmann constant, N_{tot} is the total number of vapor molecules in the bubble due to the condensation and evaporation, T_{b} is the temperature of bubble contents and R_{eq} is the equilibrium radius of the bubble.

Other important parameters for numerical simulation of bubble motion are the mass diffusion and non-equilibrium phase change of water vapor during the sonication in water. In 2000, Storey and Szeri [16, 19] proposed a two-step process that consisted of the diffusion of vapor molecule to the bubble wall and the condensation of vapor at the bubble wall, along with three important time scales, namely, the time scale of bubble dynamics (t_{osc}), the time scale of mass diffusion (t_{dif}) and the time scale of condensation (t_{cond}) as follows:

$$\begin{aligned}t_{osc}&=\frac{R}{|dR/dt|}\\t_{dif}&=ReSc\frac{R^2}{D^M_{\mathrm{H_2O}}}\approx ReSc\frac{1}{R\sqrt{T_b}},\quad Re=\rho_0R_0v_0/\mu_0,\quad Sc=\mu_0/\rho_0D_{avg}\\t_{cond}&=\frac{R}{\sigma}\sqrt{\frac{2\pi M_{\mathrm{H_2O}}}{9M_0T_0}}\end{aligned} \tag{1.6}$$

where T_{b} is the temperature of the bubble, $D^{\mathrm{M}}_{\mathrm{H_2O}}$ is the diffusion coefficient of water vapor in the gas mixture, Re and Sc are Reynolds number and Schmidt number, respectively. In Eq. 1.6, ρ_0, R_0, v_0 and μ_0 are the initial values of liquid density, bubble radius, bubble wall velocity and gas viscosity, respectively. D_{avg} is the

average binary coefficient matrix of the diffusion coefficients of vapor mixture, which is dimensionless. T_0 is the temperature of the bubble interface and the M_{H_2O} and M_0 are the molecular mass of water and the initial molecular mass of the bubble contents, respectively.

For mass diffusion of water vapor, in the earlier phase of bubble collapse, $t_{osc} \gg t_{dif}$, t_{cond}, so that bubble motion is slow enough to allow the completion of one cycle of mass transfer between liquid and bubble interior, which results in uniform bubble composition [18, 19]. Then, with the acceleration of the bubble wall, $t_{osc} \ll t_{dif}$, the bubble motion is so rapid that the water vapor has insufficient time to diffuse to the bubble wall that results in nearly unchanged composition of vapor content in the bubble [18, 19].

For condensation of water vapor, if $t_{osc} \gg t_{cond}$, the condensation is in quasi-equilibrium with respect to the bubble motion. If $t_{osc} \ll t_{cond}$, the phase change will be non-equilibrium, which results in the entrapment of water molecules in the bubble [18, 19]. However, Storey and Szeri [19] demonstrated that the condition $t_{osc} \ll t_{dif}$ is reached well before $t_{osc} \ll t_{cond}$ during bubble collapse and so the slow mass diffusion is responsible for trapping water vapor in the bubble.

Actually, during bubble oscillation, the surface temperature of the bubble exceeds the temperature of bulk water only for a very brief moment [17, 18]. Therefore, the bubble is divided into two parts, a "cold" boundary layer in thermal equilibrium with liquid and an eventually hot homogeneous core. Based on this assumption, the instantaneous diffusive penetration depth l_{dif} is taken to be Eq. 1.7 [17, 18]:

$$l_{dif} = \sqrt{Dt_{osc}} \tag{1.7}$$

where D is the diffusion coefficient.

The analysis [17] shows that the penetration depth exceeds the bubble radius ($l_{dif} \geq R$) during the expansion and a major part of the afterbounce in bubble motion, and the total volume of bubble interior is in equilibrium with the liquid. Since l_{dif} is only 0.01R during bubble collapse, this implies that the thickness of the boundary layer is negligible compared with the total bubble volume. Therefore, the bubble can be regarded as being homogeneous in both cases, and then the rate of change of water molecules in the bubble (N_{H_2O}) when the velocity of the bubble wall is non-zero is given by Eq. 1.8 as:

$$\frac{dN_{H_2O}}{dt} = 4\pi R^2 D \frac{\partial C_{H_2O}}{\partial r}|_{r=R} \approx 4\pi R^2 D \left(\frac{C_{H_2O,eq} - C_{H_2O}}{l_{dif}} \right) \tag{1.8}$$

where C_{H_2O} and $C_{H_2O,eq}$ are the actual concentrations of water molecules in the bubble core and the equilibrium concentration of water molecules at bubble wall, respectively. The $C_{H_2O,eq}$ is calculated from the vapor pressure of water at bulk temperature (T_l).

At the instant that the bubble stops growing, the velocity of the bubble wall is zero, and the upper limit of the diffusion length can be calculated [17, 18]:

$$l_{dif} = \min(\sqrt{Dt_{osc}}, \frac{R}{\pi}) \tag{1.9}$$

For diffusion of heat in analogy with diffusion of mass, in the earlier phases of bubble collapse when the time scale of bubble oscillation is longer than that for heat transfer, sufficient heat transfer helps to keep the bubble interior at ambient liquid temperature, while during bubble collapse, the bubble motion is so rapid that bubble collapse behaves nearly adiabatically with negligible outflow of bubble energy [19]. Equation 1.10 provides a method to estimate the rate of heat loss across a bubble wall during its motion [17, 18]:

$$\begin{gathered} \frac{dQ}{dt} = 4\pi R^2 \lambda_{tc}\left(\frac{T_0 - T}{l_{th}}\right), \quad l_{th} = \min(\frac{R}{\pi}, \sqrt{\frac{R\kappa}{|dR/dt|}}), \\ \kappa = \frac{\lambda_{tc}}{\rho_{mix} C_{p,mix}}, \quad \rho_{mix} C_{p,mix} = \sum_{i=1}^{n} \rho_i C_{pi} \end{gathered} \tag{1.10}$$

where λ_{tc} is the thermal conductivity of bubble contents and T_0 is the temperature of the cold bubble surface that is nearly the same with the temperature in the liquid. In Eq. 1.10, l_{th} is the thermal diffusion length, κ is the thermal diffusivity and terms ρ_i and C_{pi} are the density and molecular specific heat of compound i, respectively. The ρ_{mix} and $C_{p,mix}$ in Eq. 1.10 are the density and molecular specific heat of the vapor mixture in the bubble, respectively.

The overall energy balance for the bubble as an open system can be written as Eq. 1.11 [18]:

$$\frac{dE}{dt} = \frac{dQ}{dt} - \frac{dW}{dt} + h_{H_2O}\frac{dN_{H_2O}}{dt} \tag{1.11}$$

where dW/dt refers to the work done by the bubble. The enthalpy per water molecule that condenses at the cold bubble surface is given by $h_{H_2O} = 4kT_0$, where k is the Boltzmann constant. Equation 1.11 can be rewritten as [17, 18]:

$$\begin{gathered} C_{v,mix}\frac{dT}{dt} = \frac{dQ}{dt} - P_i\frac{dV}{dt} + \left(h_{H_2O} - U_{H_2O}\right)\frac{dN_{H_2O}}{dt} \\ U_{H_2O} = \frac{\partial E}{\partial N_{H_2O}} = N_{H_2O}kT\left(3 + \sum \frac{\theta_i T}{\exp\left(\theta_i/T\right) - 1}\right) \\ C_{v,mix} = \sum_{i=1}^{n} C_{v,i}N_i \end{gathered} \tag{1.12}$$

where U_{H_2O} is the internal energy, namely, the specific energy of water molecules in the bubble, P_i is the pressure in the bubble interior, θ_i is the characteristic vibrational temperature of species i, N_i is the number of molecules of component i and $C_{v,i}$ and $C_{v,mix}$ are the specific heats of individual component i and the mixture, respectively.

Equation 1.12 can be used to estimate the temperature change of a bubble during its motion, and it gives better results in the numerical simulation of the sonochemical phenomena [17].

In summary, cavitation behavior of a single bubble under a high intensity ultrasonic field has been discussed along with fundamental relationships. Information on the formation, growth, collapse and energy change of single bubble as the result of certain ultrasonic field parameters in a sonochemical reactor has been highlighted. By solving related mathematical equations, the motion and energy behavior of a single bubble can be estimated theoretically. By trapping a single bubble of gas in partially degassed liquid by a standing acoustic wave and then driving it into highly nonlinear oscillation, single bubble cavitation can be realized and studied in the laboratory [20], which demonstrates that cavitation takes place when the acoustic intensity is higher than the Blake threshold, and it provides much higher energy intensity than conventional acoustic streaming. The energy intensity of cavitation bubble depends on the compression ratio of bubble radius and also the net heat capacity of the bubble content. However, the entrapment of solvent vapor in the bubble at the moment of collapse consumes the heat capacity of the bubble through evaporation, which lowers the temperature attained at the moment of minimum radius during collapse. Moreover, dissociation of solvent vapor mainly involves endothermic reactions that further consume energy and contribute to the lowering of the peak temperature attained at collapse.

1.2.2 Multibubble Cavitation

In an actual sonochemical reaction, there are numerous active bubbles (ca. 10^4 bubbles/1 mL water) for sonication at 20 kHz [2]. Bubbles at different positions of acoustic field follow different cavitation behavior and have different cavitation energy due to spatial diversity of the acoustic pressure intensity. Bubble behavior is influenced not only by the acoustic field, but also by the cavitation behavior of neighboring bubbles. As a result, multibubble cavitation shows statistical results of cavitation behavior and gives rise to the interactions between bubbles.

In multibubble cavitation, the intensity and efficiency of acoustic cavitation is determined by the number density of effective bubbles in the liquid. Rectified diffusion, bubble coalescence and concerted collapse influence the behavior of bubbles.

Rectified diffusion. In acoustic cavitation, two possibilities exist for the newly formed bubble nuclei—dissolution in the liquid phase if the ultrasonic intensity is below a threshold value, or growth to a larger size under the action of negative acoustic pressure. If the size of the bubble expands to over a critical (resonance) size, the bubbles will quickly collapse in the following positive acoustic pressure stage, which initiates sonochemical reactions. However, several or tens of acoustic cycles may be necessary for a significant number of bubbles to reach the critical size (Fig. 1.4) [21]. Rectified diffusion is the main way to enlarge the sizes

of bubbles to a critical size, whether in single bubble cavitation or in multibubble cavitation. Rectified diffusion refers to the unequal mass transfer through the cavitation bubble wall in an acoustic cycle. In the expansion phase of bubbles, gas concentration in the bubbles decrease, which drives the mass transfer from bulk liquid to bubble interior. During the shrinkage of bubbles, materials in the bubbles diffuse out of the bubbles. The expansion process of bubbles is relatively slow, while shrinkage of bubbles is rapid. In bubble expansion, the surface area of the bubble is much higher than that during shrinkage. Volumetric work done by the shrinkage of bubble is converted to the evaporation heat of liquid molecules at the bubble/liquid boundary, namely more liquid molecules transform into vapor content of the bubble. Since materials flowing into the bubble are more than materials flowing out in the acoustic cycles, net growth of cavitation bubbles occurs [21].

Bubble coalescence. Compared with the slow progress of rectified diffusion, bubble coalescence can be regarded as a rapid progress in which bubbles grow to the critical size. Bremond et al. [22] used photography that showed the coalescence of two bubbles subjected to a negative pressure of −2 MPa. The work demonstrated that if the distance of two bubbles is in the range for weak interaction (400 μm for instance), collapse of the two bubbles will be delayed due to the partially shielding of acoustic pressure by each other, but the coalescence would not occur. However, if the two bubbles are initially closer to each other (ca. 200 μm), or if the intensity of negative pressure increases, the two bubbles will lose their spherical shape and join to form a single bubble. The significant interaction of cavitating bubbles with their neighbors is governed by secondary Bjerknes forces derived from the nonlinear oscillations of bubbles [23, 24]. A threshold distance exists for the merging of bubbles. The secondary Bjerknes forces become dominant and attract two bubbles to move towards each other only when the distance of the two bubbles is within a threshold value [23]. High acoustic pressure accelerates the approach and merging of bubbles. The threshold distance is 200 μm when the acoustic pressure is 10 kPa, while it increases to 500 μm when the acoustic pressure is 40 kPa [23]. Bubble interactions reversely affect the nonlinear motions of each bubble and thus influences cavitation phenomena and sonochemical yields [24].

An interesting work on the experimentally observation and control of bubble coalescence was performed by Ashokkumar [15] and Ashokkumar et al. [21]. They used pulse ultrasound instead of continuous ultrasound. The growth of bubbles in the measuring system was stimulated when the ultrasound was applied, however, during the off time, some small bubbles became dissolved in the liquid, while others that had sizes large enough to live through the pulse off period, continued to grow in the next acoustic pulse. As mentioned before, most bubbles need several or tens of acoustic cycles to reach the critical size, which is also referred to as an "induction period" for the achievement of steady cavitation. As shown in Fig. 1.4b, the number of acoustic pulses required for steady cavitation in water under a pulse ultrasonic field at 515 kHz is about 10, while with the addition of surfactants—methanol (Fig. 1.4c) and sodium dodecyl sulfonate (SDS, Fig. 1.4d), the number of acoustic pulses increases to about 20 and 40, respectively. The addition of surfactants seems to change the surface properties of the bubbles, and

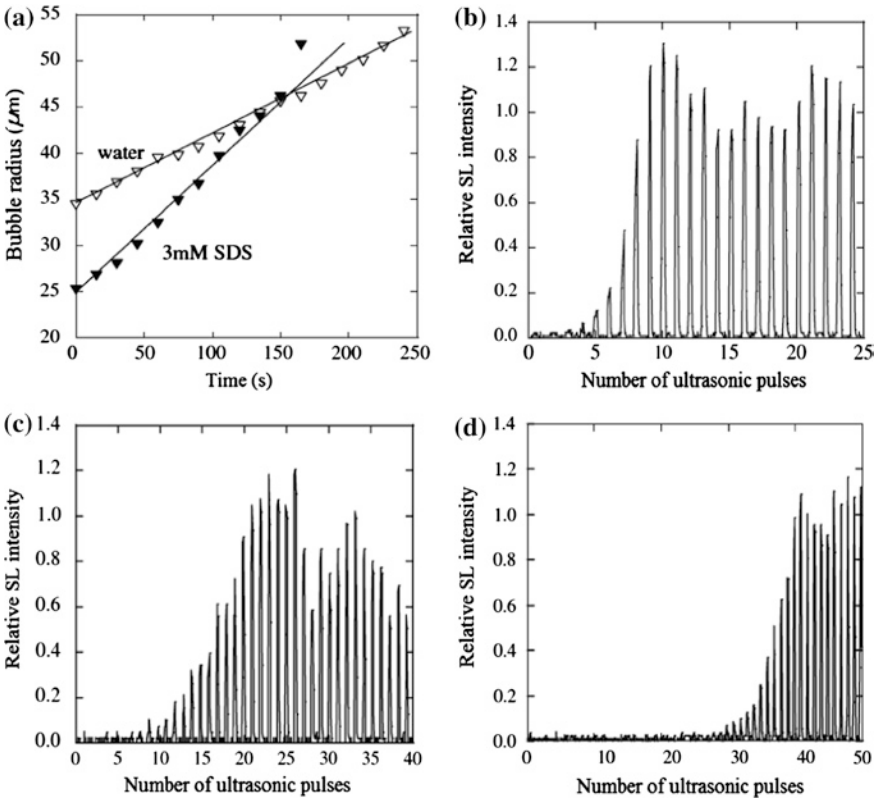

Fig. 1.4 Bubble growth in surfactant solution under sonication: **a** bubble growth as the function of time in water and sodium dodecyl sulfonate (*SDS*) solution at acoustic pressure of ~0.022 MPa and frequency of ~22 kHz; **b** sonoluminescence (*SL*) intensity as the function of acoustic pulse number in water under pulse ultrasonic field at 515 kHz; **c** SL intensity as the function of acoustic pulse number in 1 M aqueous methanol solution under pulse ultrasonic field at 515 kHz; **d** SL intensity as the function of acoustic pulse number in 0.75 mM aqueous SDS solution under pulse ultrasonic field at 515 kHz (adapted with permission from [21], Copyright © 2007 Elsevier)

hinders coalescence of small bubbles to larger ones. As a result, the growth of bubbles through bubble coalescence requires more sonication time or more acoustic pulses in surfactant solutions. On the other hand, for high concentration of SDS, the adsorption of SDS at the bubble/liquid interface is thought to restrict outflow of chemical matters in the bubbles during bubble shrinkage. Therefore, the growth of bubbles via rectified diffusion route is promoted and accelerated with the addition of surfactants.

Concerted collapse. In a bubble cloud, the collapse of a bubble emits strong shockwaves. The produced shockwave elevates the ambient pressure or external energy intensity on neighboring bubbles, and accelerates the collapse of neighboring bubbles and other bubbles in the cloud. This assumption is referred to as

concerted collapse [2, 25]. Concerted collapse starts at the boundary of a bubble cloud and proceeds until collapse of bubbles at the cloud center occurs. As a result, shockwaves from multiple bubbles converge together and form a single shockwave directing towards the solid surface with much higher shockwave intensity (several hundreds of kPa) than the collapse of multiple single bubbles.

In a practical sonochemical reactor, the behavior of bubbles is influenced by the pattern of ultrasonic streaming. Some sonochemical systems show interference characteristics in ultrasonic wave propagating in the whole reactor space, which means numerous alternate or fixed regions with strong or weak ultrasonic intensity. An example is the common ultrasonic bath with special depths (integral multiples of quarter-wavelength of ultrasound wave) from the bath bottom to the liquid surface. For this type of sonochemical reactor, the collapse of bubbles are generally concentrated at points that have high ultrasonic intensity (antinodes) in the reactor space, which gives high cavitation activities as shown in Fig. 1.5 [26, 27]. Regions with long-term low or even zero ultrasonic intensity (nodes) may favor the growth of bubbles via rectified diffusion and coalescence. At these nodes, the size of the bubbles may increase beyond the critical size. The bubbles possibly survive even for long time after the ultrasound is shut off [21]. The behavior of bubbles at antinodes or nodes is also used in distinguishing the intensification mechanism of cavitation from that of ultrasonic streaming [28].

Because of the uncertainties in the spatial distribution of bubble size and bubble density as well as the complex interaction between bubbles, the determination of cavitation in a multibubble system is more involved than that for a single bubble system [15, 20]. Several effective methods have been developed for analyzing cavitation in multibubble systems [14, 15, 29, 30]. These methods are summarized in Table 1.2. Acoustic frequency spectroscopy (AFS, Fig. 1.6) is

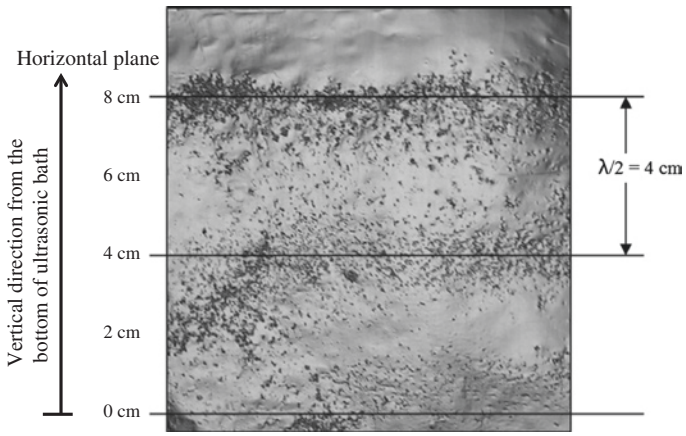

Fig. 1.5 Cavitation erosion pattern on aluminum foil vertically positioned in ultrasonic bath (water depth of 10 cm) at 20 kHz (adapted with permission from [27], Copyright © 2009 Elsevier)

Table 1.2 Qualitative and quantitative approaches for measuring ultrasonic cavitation and secondary effects

Method	Sensor	Principle of measurement	Reference
Spectroscopic			
Acoustic frequency	Hydrophone	Steady and transient bubbles oscillating at subharmonics, harmonics and ultraharmonics frequencies produce variation of local acoustic pressure	[27, 31]
Sonoluminescence	Light intensity	Light intensity is detected and plotted as the function of scanning wavelength from 300–900 nm (ultraviolet-visible range)	[14, 15, 29]
Chemical			
Iodine method	·OH radical	$H_2O \rightarrow \cdot OH + \cdot H$, $I^- + \cdot OH \rightarrow I_2^- \rightarrow I_3^-$ I_3^- concentration determined by ultraviolet spectroscopy	[30]
Fricke method		$H_2O \rightarrow \cdot OH + \cdot H$, $Fe^{2+} + \cdot OH \rightarrow Fe^{3+} + OH^-$ Fe^{3+} concentration determined by ultraviolet spectroscopy	
Salicylic acid method		Hydroxylation of salicylic acid by ·OH radical Salicylic acid concentration determined by high performance liquid chromatography	
Terephthalic acid method		*p*-$C_6H_4(COOH)_2 + \cdot OH \rightarrow C_6H_3OH(COOH)_2$ Hydroxyterephthalic acid concentration determined by fluorescence spectroscopy	
Sonochemiluminescence		3-Aminophthalhydrazide (luminol) + ·OH → 3-aminophthalate, in alkaline solution Blue light emission of 3-aminophthalate proportional to concentration	
Physical			
Aluminum foil erosion	Al foil	Indentations on foil and weight loss	[27, 30]
Laser scattering	Light attenuation	Volumetric concentration of bubbles from Beer-Lambert law	[32, 33]
Laser phase-Doppler	Frequency variation	Velocity of bubbles from frequency variation between scattering and incident waves while bubble size by phase displacement between scattering and reflected waves	[33, 34]

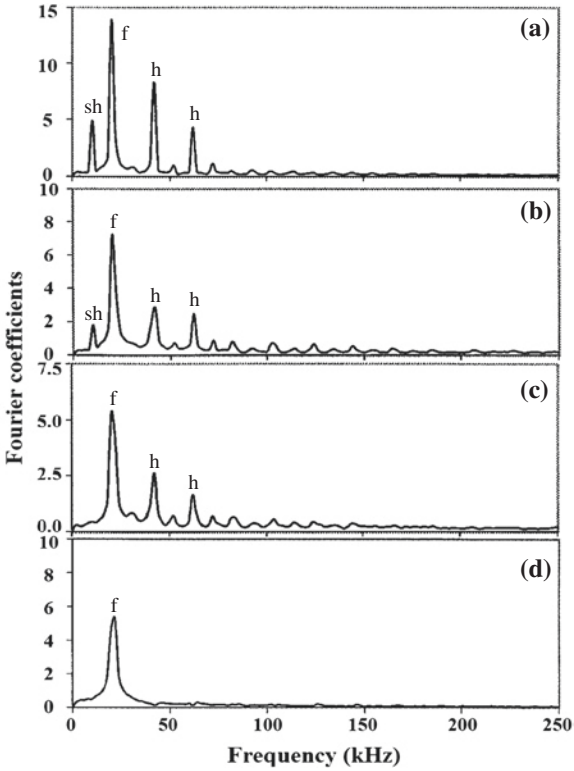

Fig. 1.6 Average acoustic frequency spectra under sonication of 22 kHz: **a** strong cavitation intensity in water; **b** medium cavitation intensity in water; **c** weak cavitation intensity in water; **d** no cavitation intensity in silicon oil. *f* fundamental frequency (22 kHz); *h* harmonic frequencies; *sh* subharmonic frequencies (adapted with permission from [31], Copyright © 2000 American Institute of Chemical Engineers [AIChE])

a direct but approximate way for measuring the occurrence of acoustic cavitation. Hydrophones are placed in liquid under sonication, and record the intensity of pressure pulse at local place as the function of scanning frequency. AFS results reflect the change of acoustic parameters as the result of acoustic activation. Since it uses hydrophones for detection of sound waves, AFS needs complex mathematical transformation and processing to obtain useful information from the as-received spectra [27]. AFS spectrum with high intensity peaks at the harmonic, higher harmonic, or even subharmonic frequencies proved the occurrence of cavitation [27, 31]. Chemical measurements are normally used in the quantitative determination of cavitation yield and cavitation efficiency [12, 30]. In common horn- and bath-type reactors, the cavitation yields are determined as 3.5×10^{-9} and 5.8×10^{-7} g/J, respectively, which give relatively low energy efficiency (5–20 %) of acoustic cavitation [12]. Because of less energy requirement, the results from chemical measurement represent the less violent energy characteristics in bubble dynamics than that from sonoluminescence [15]. Erosion analysis of aluminum foil of several micrometer thickness is used to evaluate the cavitation number (punching number on foil) and cavitation intensity (weight loss of foil).

Results from chemical methods and erosion analysis describe the intensity of ·OH radical and shockwave, secondary effects of cavitation, respectively.

Advanced technologies such as pulsed multibubble sonoluminescence (MBSL), laser diffraction [32, 33], laser phase-Doppler [33, 34], methyl radical recombination and others are widely used in analyzing multibubble cavitation in recent years, and these methods give the scale or distribution of energy, number, size, velocity of bubble clusters. For MBSL, light emitted at certain wavelength relates to the formation of special plasma. Light intensity is proportional to the energy intensity of bubbles. By fitting the emission spectra of special plasma, the emission temperature of plasma in bubbles can be estimated, which indicates the energy level of bubble cavitation. However, the analysis of multibubble cavitation is still challenging. In fact, as the time for bubble collapse is short, cavitation bubbles analyzed by various methods are mainly in growth or in oscillating, which does not apply to the bubbles before collapse. For laser phase-Doppler, the number and volume factions of bubbles are plotted against to the motion velocity and size of bubbles at certain plane in acoustic field. Velocity of bubbles is determined by frequency variation between scattering and incident waves, while bubble size is determined by phase displacement between scattering and reflected waves. Laser scattering and laser phase-Doppler are both direct methods to determine the cavitation number.

In multibubble cavitation, the production of cavitation bubbles means the formation of another immiscible phase besides the liquid medium. The intensity of ultrasonic energy is scattered and weakened for a heterogeneous liquid containing high concentrations of insoluble solid particles or gas microbubbles. High acoustic intensity produces high number density of bubbles (bubble cloud) in the liquid phase, while high number density of bubbles greatly influence the delivery of acoustic intensity to the entire reactor space. These two opposing effects have contradictory consequences [26]. For example, in a horn type sonochemical reactor, a high density of bubble cloud gathers at the region near the tip of the transducer, and results in inefficient cavitation in sonochemical processing [35]. Thus, the system with a controlled concentration of cavitation nuclei gives much higher cavitation intensity than the system with too many nuclei and the system suffering completely denucleation [26]. Appropriate number of cavitation nuclei uses energy efficiently.

The formation and distribution of cavitating bubbles in the whole space of a sonochemical reactor is not uniform and is greatly influenced by ultrasonic streaming. Ultrasonic streaming occurs according to the geometry of the reactor and the variation of its ultrasonic parameters. By using high-speed photography [36] and chemical methods such as the iodine method [37] and sonochemiluminescence [38], it is possible to observe and record the spatial distribution of active bubbles. Bubbles are forced to migrate directionally in the acoustic field due to primary Bjerknes forces. The primary Bjerknes force is defined as the translational force on a cavitating bubble in a liquid when the nonlinear oscillation of the cavitating bubble is interacting with the acoustic pressure field [39]. Parlitz et al. [40] demonstrated that when the amplitude of the acoustic pressure was not high, cavitating bubbles tended to move along the direction of pressure rise (pressure antinode). This deduction is consistent with the phenomenon that is described in the

section dealing with concerted collapse (Fig. 1.5). However, when the amplitude is further increased, the primary Bjerknes force may change, and the high pressure amplitude region may become repulsive for the bubbles because of nonlinear oscillation of bubbles [36, 40]. As a result, in an acoustic field near a sonotrode with the pressure amplitude of greater than 190 kPa [36], cavitation bubbles tend to move along the direction of pressure drop. This creates different spatial distributions and migration features of bubbles in a reactor that is commonly referred to as acoustic cavitation structure.

Typical acoustic cavitation structures can be conical bubble structure (CBS), smoker bubble structure, tailing bubble structure (TBS), jet-induced bubble structure (JBS) and acoustic Lichtenberg figure (ALF). Acoustic cavitation structure CBS (Fig. 1.7a) [36] and smoker (Fig. 1.7b) [41] are two common forms that

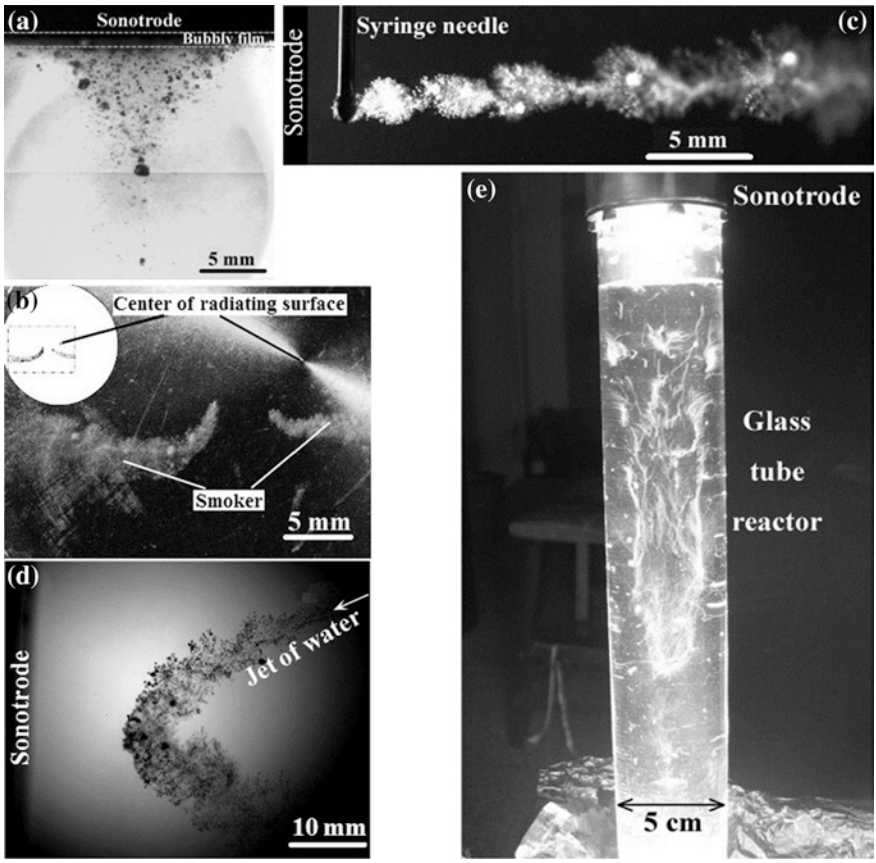

Fig. 1.7 Acoustic cavitation structures: **a** conical bubble structure; **b** smoker bubble structure; **c** tailing bubble structure; **d** jet-induced bubble structure; **e** acoustic Lichtenberg figure (**a**, **b**, **d** and **e** are reprinted with permission from [36], Copyright © 2014 Elsevier. **c** is reprinted with permission from [42], Copyright © 2014 Elsevier)

occur in a relatively strong acoustic field. CBS is produced by sonotrode. When the sonotrode vibrates with moderate amplitude, the radiating surface is covered by bubbly web structures and the CBS is composed of filament structures, while as the vibrating amplitude of the sonotrode increases, the CBS becomes a homogeneous distribution of bubbles and the radiating surface is covered by a bubbly film [36]. Smoker, which only appears on a radiating surface such as the bottom of a cleaning bath or on the surface of transducer submerged in liquid, is bound to the surface with a small tip and a big tail [41]. TBS (Fig. 1.7c) and JBS (Fig. 1.7d) are two new acoustic cavitation structures produced by artificially implanting nuclei in a strong acoustic field [42]. For TBS, acoustic radiation forces make the cavitation bubbles move away from the radiating surface to form a cloud tail [42]. For JBS, the submerged liquid jet and acoustic radiation forces both determine the direction of the bubble translation [42]. ALF (Fig. 1.7e) occurs in an ultrasonic field with relatively weak intensity [40, 43]. Bubbles in ALF translate towards the pressure antinodes one after another that causes a dendritic bubble structure and self-organization. The nuclei sources of CBS and smoker are mainly small air bubbles trapped within crevices or non-condensed air microbubbles in the liquid. The nuclei sources of TBS and JBS are small air bubbles that originate from foreign impurities or the submerged liquid jet [36]. The above acoustic cavitation structures are closely interrelated to each other and can be interchanged under special conditions. By artificially implanting nuclei, one can create controllable distributions of cavitation bubbles over an entire reactor space that is favorable for promoting sonochemical reaction [42].

In summary, this section has discussed statistical cavitation behavior of bubbles formed under the application of ultrasound to a reactor. The spatial characteristics in number density or volume fraction of bubbles with certain sizes or velocities in the uneven acoustic intensity field have been mainly considered. The number and size distribution of bubbles greatly influence cavitation behavior of neighboring bubbles and thus it strongly affects the product yields in sonochemical reactions.

1.2.3 Physical and Chemical Effects of Cavitation

The oscillation and transient collapse of cavitation bubbles produce many special secondary physicochemical phenomena, including shockwave, microturbulence, microjet, radical effects and sonoluminescence, which can have great influence on the dynamics and process equilibrium in a system. Mass and heat transfer coefficients of a reacting system can be multiplied by sonication with the predominant reason for enhancement being related to acoustic cavitation and its secondary effects [28, 44]. The collapse of transient bubbles produces local hot spots with temperature and pressure that is much higher than that of the surrounding liquid. The huge temperature and pressure drop generates strong shockwaves towards bubble outsides [45]. The shrinkage and transient collapse of bubbles creates large voids in the liquid, while the quick influx of liquid stream to the voids forms

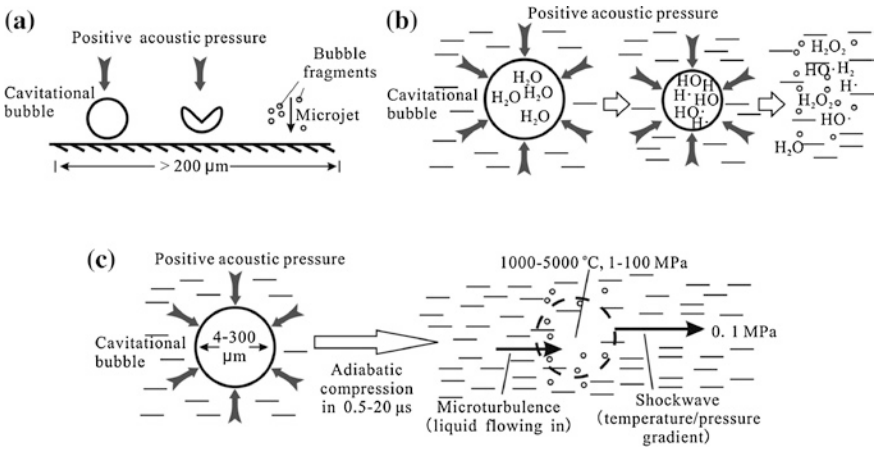

Fig. 1.8 Schematic representations of secondary effects: **a** microjet, **b** radical formation and **c** shockwave and microturbulence in ultrasonic cavitation

violent microturbulence in local liquid. Microjet refers to the unsymmetrical collapse of bubbles at a broad solid/solvent interface (>200 μm) that produces high speed impact (>100 m/s) oriented towards the solid surface [2]. Schematic representation of several secondary effects is given in Fig. 1.8. As shown in Fig. 1.1, the collapse of transient bubbles produces secondary effects that have a much higher intensity than the oscillating motion from steady bubbles [8]. Transient bubbles have a more violent change in bubble size during the acoustic cycle. Therefore, the intensities of shockwave and microturbulence emitted by transient bubbles become about 3,000 and 40 times, respectively, of that from steady bubbles (Fig. 1.1).

During cavitation, high-temperature dissociation of gaseous water molecules generates radical ·OH, while the burning of gaseous N_2 with gaseous O_2 generates ion NO_2^- in bubbles as bubbles shrink or collapse. And light is emitted from the emissive shell (sonoluminescence). In the sonication of water at 22 °C and 52 kHz, a single cavitating bubble with a maximum radius of 28.9 μm produces 6.1×10^{-18} mol NO_2^-, 1.1×10^{-18} mol ·OH and 1.3×10^{-20} mol photons in an acoustic cycle [20]. However, the negligible amounts of these spontaneous species has less influence on the performance of general sonochemistry [46].

It should be clarified that ultrasound wave, acoustic cavitation and these secondary effects have their action range. Most cavitation activity and high sonochemical yields appear within the distance of about one wavelength, namely several centimeters, away from the sound-emitting surface such as the ultrasonic horn [47, 48]. In some texts [1], according to the distance X away from the sound-emitting surface, the action zone for ultrasound in sonochemical reactor is divided as near-surface zone ($X <$ wavelength λ), streaming zone ($X \sim \lambda$) and far-field zone ($X > \lambda$). Only the near-surface zone is suitable for effective cavitation and sonochemical reactions, while the streaming zone is suitable for particle aggregation

and emulsion separation under low intensity ultrasound by standing wave principle. The action ranges of acoustic cavitation and relevant secondary effects are much shorter. The surrounding liquid absorbs much of the cavitation energy, while the reactive radicals generated by cavitation are easily quenched and cannot migrate far from the location of the collapsed bubble. The attenuation of the pressure pulse for the bubbles is greater than 5 μm, which makes the pressure amplitude measured at 1 mm from the bubble center only 10^{-3} of its actual value [31]. In a heterogeneous system, such as in systems containing a high concentration of small-size solid particles, the absorption of cavitation energy by the surroundings become significant due to the scattering effects. Near the surface of the solid materials, the shockwave that has high temperature and high pressure from bubble collapse, impacts the solid surface and changes the morphology and properties of solid surface. The high energy shockwave lasts for short time of about 200 ns and this happens within a short distance of only tens of nanometers from the solid surface [2]. However, the energy from many shockwaves can be concentrated and enhanced due to concerted collapse. Therefore, it is possibly for ultrasound wave to make indentations of 10–100 μm on solid surface even if the solid surface is exposed under acoustic cavitation for a short period of time [2].

As shown in Fig. 1.3, the active zones for acoustic cavitation and most of the derived physicochemical effects can be divided into four parts—bubble interior, bubble/liquid interface, nearby zone and far-distance zone. The bubble interior allows the access of volatile chemicals and dissolved gases. The bubble generates high temperatures and pressures in its interior during the nearly adiabatic compression process, and initiates ionization, thermolysis and violent radical reactions of vapor molecules. Radical reactions not only occur in the bubble interior, but also at the bubble/liquid interface and in the nearby liquid, especially for nonvolatile compounds. In the sonochemical degradation of phenol in water, the increase of relative concentration of nonvolatile phenol at the bubble/liquid interface promotes the degradation efficiency of phenol multiply even though the concentration of phenol in the bulk liquid remains almost unchanged [49]. This demonstrates that the bubble/liquid interface plays a vital role in radical-induced chemical reactions of nonvolatile compounds under sonication. However, it does not mean that the chemical reactions of nonvolatile compounds cannot take place in the bubble interior. In the study of sonoluminescence in concentrated H_3PO_4 solution, peaks assigned to radicals ·OH and PO· are both significantly visible in the ultraviolet spectrum [29]. In the sonoluminescence of H_3PO_4, radical PO· must be produced from nonvolatile H_3PO_4 in the plasma zone, namely the deepest core in the bubble structure. There are probably two different types of cavitating bubbles that exist in sonicated H_3PO_4 solution [29]: (1) stationary bubbles that undergo highly symmetrical collapse and produce radical ·OH and (2) rapidly moving bubbles that have less symmetrical collapse. In the second type of bubbles, nanodroplets of liquid containing H_3PO_4 might be injected into the bubble interior due to capillary wave action, microjetting, or bubble coalescence in the asymmetry collapse of bubbles [29]. However, the ratio of chemical reactions of nonvolatile species in bubbles is not large. As the collapse of transient bubble occurs, numerous active

radicals are released into the nearby liquid which initiate radical reactions such as the oxidative degradation of chemical materials in wastewater or are captured by chemical reagent in determining cavitation activity. For the nearby zone which is within 100 μm from the bubble boundary, the dominant ultrasound-intensification mechanism is physical, such as shockwave and microturbulence. High impact and high temperatures that result from shockwave and high-speed microjet are responsible for the modification of solid surfaces under high-energy ultrasound, such as surface erosion, particle breakage, metal melting and peeling of surface oxide coating [2, 50]. Microturbulence promotes dispersion and fine emulsification in immiscible liquid mixtures and helps to dislodge substances that adhere onto solid surfaces (ultrasonic cleaning). In the far-distance zone, cavitation and shockwaves lose their strength, while microturbulence may be the main mechanism for ultrasonic intensification of chemical processing such as emulsification [48].

Most sonochemical reactions do not occur in the interior of active bubbles. The intensification of these sonochemical reactions is through the action of secondary effects, but not the cavitation behavior of bubbles themselves. However, the energy intensity of secondary effects greatly depends on the behavior of the bubbles, as well as the liquid properties and heterogeneous characteristics of the reaction system. For chemical reactions that are related to biomass conversion, the effective intensification/activation zones are mainly the zones that are nearby the bubbles and the zones that have distance within one wavelength from the bubbles. Therefore, the physical mechanism should be applicable to the discussion of ultrasound-enhanced biomass processing, and intensification of the mass transfer.

1.2.4 Factors that Influences the Energy of Acoustic Cavitation

For most practical sonochemical reactions, it is necessary to know the factors that could influence acoustic cavitation, and these factors include the physicochemical properties of liquids, acoustic operation and heterogeneous characteristics of reaction system [4, 5, 51, 52]. The selection and optimization of those factors allows proper energy intensity to be applied and gives higher energy efficiency. Table 1.3 describes some important factors and their effects on cavitation. Energy efficiency for cavitation is related to the proper design of sonochemical reactors that provide a uniform acoustic energy field for bubble cavitation. Generally, the influence of the factors shown in Table 1.3 can be divided into four categories:

1. **Influence on acoustic environment for the occurrence of cavitation**. Factors such as heterogeneous characteristics, acoustic frequency and liquid temperature influence the propagation and attenuation of acoustic energy in the liquid and thus affect the intensity and uniformity of the acoustic field. The characteristics of acoustic streaming in different reactors also influences the spatial distribution of acoustic energy [54].

2. **Influence on the occurrence of cavitation, namely cavitation threshold and cavitation density**. Dissolved gases and volatile liquids provide cavitation nuclei, which lower cavitation threshold and make the occurrence of cavitation easier. Relatively high acoustic frequency increases the number of useful cavitation events in per unit of time by shortening the duration of an acoustic cycle.
3. **Influence on growth and energy accumulation of bubbles**. High acoustic frequency reduces time for the expansion and compression of bubbles, and influences the work done onto the bubble during compression and the energy concentration generated thereby. The properties of liquids such as surface tension and viscosity limit the growth and maximum size of bubbles. The concentration of organic liquids and surfactants influences the growth of bubbles through rectified diffusion and bubble coalescence.
4. **Influence on the release of bubble energy during their shrinkage and collapse**. The evaporation of liquid in bubbles and the chemical reactivity of liquid and dissolved gases both consume the energy obtained during bubble growth and these buffer the released intensity of cavitation and the secondary effects [53]. Heterogeneous characteristics and high viscosity in liquid absorb the intensity of secondary effects and result in their rapid reduction.

Many factors may promote acoustic cavitation in one aspect but may have adverse effects on another aspect. Representative cases appear in the discussion of acoustic frequency [51] and bubble cloud effects [26], which are mentioned in Table 1.3 and Sect. 1.2.3, respectively. Thus comprehensive analysis and evaluation of the factors influencing acoustic cavitation (Table 1.3) is needed. For practical sonochemical processes, the purpose of chemical treatment often determines the selection and optimization of ultrasonic parameters [51]. High ultrasonic frequency of >100 kHz weakens the physical or mechanical effects generated by acoustic cavitation [55], however, it promotes advanced oxidation reactions through radical reaction pathways [56]. Furthermore, the conditions with the highest cavitation efficiency are not necessarily the optimal conditions for achieving highest product yields in sonochemical reactions. The best of reaction temperature must be appropriate for both cavitation effects and the chemical dynamics [51].

The heterogeneous characteristics in cavitating systems are especially important. Strictly speaking, no cavitation happens in an absolutely single phase. Even for acoustic cavitation mediums such as concentrated H_2SO_4 or H_3PO_4 solution or ionic liquids that have a very low vapor pressure, the cavitating system is heterogeneous [29, 57–59]. Much of the literature has demonstrated that high cavitation intensity can be obtained with only very small numbers of bubble nuclei. More importantly, compared with water and common organic liquids that have high volatility, cavitation in low-vapor-pressure and nonpolyatomic vapor liquids such as concentrated H_3PO_4 solutions reduces excessive energy consumption due to solvent evaporation, polyatomic vibrations, rotations, and especially endothermic bond dissociations. As a result, high cavitation intensity is obtained in concentrated H_3PO_4 solutions, which emits bright MBSL intensity that could be visible under fluorescent lamp [29].

Table 1.3 Factors influencing acoustic cavitation [4, 5, 51–53]

Factor	Direct effect	Remarks
1. Liquid properties		
Compressibility	Cavitation bubble dynamics	High compressibility reduces cavitation intensity
Vapor pressure	1. Cavitation threshold 2. Vapor composition in bubble 3. Intensity of bubble collapse	High vapor pressure makes cavitation easier, but decreases energy intensity of bubble collapse due to liquid evaporation during acoustic cycles
Surface tension	1. Cavitation threshold 2. Bubble size	High surface tension increases cavitation threshold, but gives bubble collapse with high energy intensity
Viscosity	1. Cavitation threshold 2. Bubble oscillation	1. Cavitation occurring in low viscosity is mainly transient
		2. High viscosity induces steady or no cavitation. High cavitation energy in single bubble and high attenuation of acoustic energy, shockwave and microturbulence
Chemical reactivity	1. Radical formation 2. Intensity of bubble collapse	Reaction of active compounds consumes the energy released by cavitation
Pretreatment	Cavitation threshold	Degassing and nucleation influence acoustic cavitation
2. Properties of gas in liquid		
Gas solubility	1. Number of cavitation events 2. Vapor composition in bubble	1. Dissolved gas acts as cavitation nuclei facilitating cavitation 2. Cavitation intensity is inversely proportional to amount of dissolved gas
Specific heat, thermal diffusivity	1. Heat transfer between bubble and liquid 2. Energy of cavitation bubbles	Low thermal conductivity of gas leads to high local heating during bubble collapse
Chemical reactivity	1. Radical formation 2. Intensity of bubble collapse	Reaction of compounds decreases the energy intensity of bubble collapse
3. Liquid temperature		
	1. Bubble dynamics 2. Liquid properties, gas solubility 3. Sound propagation	1. Complex influences. Liquid temperature increases cavitation intensity due to volatility effect in most cases 2. Chemical reactions need appropriate temperature for efficient coupling of cavitation effects with chemical dynamics
4. Static pressure		
	1. Cavitation threshold 2. Bubble dynamics	High cavitation threshold and violent bubble collapse occur at high static pressure
		Increasing static pressure allows one to distinguish between acoustic microstreaming and cavitation mechanism
5. Existence of solid particles		
	1. Spatial distribution of acoustic intensity 2. Intensity of secondary effects	High concentration of solid microparticles decreases cavitation efficiency and intensity of secondary effects due to acoustic scattering

(continued)

Table 1.3 (continued)

Factor	Direct effect	Remarks
6. Acoustic intensity		
	1. Bubble dynamics 2. Number of cavitation events	1. High acoustic intensity promotes cavitation 2. Capacity for indefinite increase of acoustic intensity depends on material stability of transducer and the properties of liquid medium. Acoustic intensity is determined according to reaction requirement 3. Bubble cloud effect seriously decreases cavitation efficiency at high acoustic intensity. Additional auxiliaries such as mechanical agitation avoid bubble clouds gathering in zones that have high acoustic intensity
7. Acoustic frequency		
	1. Acoustic cycle 2. Bubble dynamics 3. Cavitation threshold 4. Sound attenuation	1. Cavitation threshold increases with acoustic frequency 2. High acoustic frequency of >1 MHz means short acoustic cycle and insufficient time for the generation, growth and collapse of bubbles 3. High frequency increases attenuation of ultrasonic energy in liquid 4. Number of useful cavitation events per unit time increases for acoustic frequency of <200 kHz. This increases cavitation efficiency 5. Longer duration of bubble motion and larger bubble size exist with low frequency. This increases the evaporation of liquid at the bubble surface and chemical reaction of vapor content in bubble, which consumes energy in cavitation bubble, and decreases the energy intensity of transient collapse

It can be concluded that in "homogeneous" liquids, the concentration of microbubbles that are artificially produced by researchers determines the cavitation intensity in sonochemical reactors. This conclusion is obtained for microbubbles from vapor that is produced by solvent volatilization, but the conclusion is also applicable to liquid containing noncondensable gases. In the latter case, noncondensable gases displace vapor molecules as the main source of microbubble nuclei, while the content of noncondensable gases in liquids can be controlled by properly degassing and removal of gas microbubbles trapped in crevice (denucleation) [26]. Aqueous solutions that are not degassed give relatively poor cavitation intensity according to acoustic emission spectrum results, and this is due to the acoustic attenuation and acoustic energy scattering in the bubble-rich liquid. Aqueous solutions that are completely pre-denucleated show no cavitation intensity as no microbubble is available as cavitation nuclei. As a result, the highest

acoustic emission intensity is observed in the liquid that is degassed but not denucleated which contains a controlled concentration of noncondensable air [26]. In most cases, degassing before sonochemical treatment enhances the intensity of cavitation and dramatically improves cavitation distribution. Cavitation is concentrated more closely to transducers when sonication is performed in tap water, while it is highly dispersed and evenly in the whole reactor space when sonication is performed in boiled water [60]. Nuclei concentration effects seem to artificially regulate cavitation intensity in homogeneous liquids.

For solid-liquid heterogeneous systems, especially patterned geometry of defects on solid surfaces, the size and concentration of the solid micro-/nanoparticles are important for selective production or control of cavitation intensity [6, 7]. As mentioned in Sect. 1.2.1, smart design of surface defects can enhance the nucleation rate by several orders of magnitude [6]. In biomass reactions handing lignocellulose particles, appropriate particle size (several tens to several hundreds of micrometers) [61, 62] and solid concentration (<5 wt%) [51] seems to promote efficient reaction.

Another interesting heterogeneous system is the hot-pressed solvents such as subcritical CO_2 [63]. Acoustic cavitation only occurs below the critical point of liquid, because no phase boundary exists above the critical point. Compared to ambient water, acoustic cavitation in subcritical CO_2 requires a lower threshold pressure, as the high vapor pressure of CO_2 counteracts the hydrostatic pressure. The Blake threshold for subcritical CO_2 at 20 °C and 5.82 MPa is only 0.1 MPa, while water needs 5.9 MPa for the same conditions [63]. Theoretical calculations show that with stimulation of ultrasound at 20 kHz, liquid CO_2 at 20 °C and 5.82 MPa gives high cavitation intensity, with the maximum bubble radius comparable to that in water at 20 °C and ambient pressure [63]. The acoustic cavitation in subcritical CO_2 is already used in radical-induced chemical reactions, such as polymer synthesis.

1.3 Conclusions and Future Outlook

Ultrasound can be an effective technology for process intensification by acoustic cavitation in many chemical reactions. Acoustic cavitation accumulates and explosively releases energy through the growth, radial motion and collapse of bubbles. The intensity of released energy is enough to break chemical bonds and even to generate plasma and photons. However, in many practical reactions, secondary effects generated by cavitation become the primary and direct cause for process intensification under sonication, while the intensity of secondary effects also depend on the behavior of bubbles themselves and the influence from the properties of the sonication medium. The analysis of influencing factors must be comprehensive and be directed towards specific situations. Ultrasonic streaming and heterogeneous characteristics of sonochemical systems have great influence on the efficiency of acoustic cavitation, namely the transformation ratio of ultrasonic

energy to cavitation energy. Some qualitative and quantitative approaches are recommended for measuring ultrasonic cavitation and secondary effects, which will help to understand the regularity of cavitation energy and its distribution in specific reactors. Optimization of chemical reactions under sonication can be achieved through combined knowledge of the regularities in cavitation energy, ultrasonic operation and reaction requirement.

Acoustic cavitation can vary greatly between reactor types and different sonochemical systems. Mechanics and fluid dynamics help to develop mathematical models for acoustic cavitation and provide some possible theoretical frameworks. However, experimental methods are needed to examine many hypotheses that are used in the design of practical reactors. In the last decade, new technologies such as multibubble sonoluminescence and advanced photography have greatly elevated the progress of experimental acoustics, and advanced application of ultrasound in biomass conversion. However, new studies are still needed to help many of the intrinsic characteristics and nature of acoustic cavitation. Research areas that are probably fruitful for exploration are: (1) acoustic cavitation in multibubble systems, (2) cavitation in special liquid mediums such as viscous liquid, ionic liquids and near-critical fluids, (3) acoustic cavitation occurring on the solid/liquid interface both on experimental and theoretical level, (4) characteristic analysis of acoustic fields in new sonochemical reactors with different geometric arrangements and (5) mechanisms of sonochemistry for special reactions.

Especially, the experimental mapping and theoretical study of the spatial distribution of active cavitation in reactor space needs more attention. Further, the combination of sonochemistry with general chemistry methods should be given attention within educational environments.

In practical chemical processes that are enhanced by ultrasonic energy, the most important consideration will be the system performance and energy efficiency of the applied ultrasound. New advances in the statistic analysis and purposeful design of the energy of cavitation bubbles will allow the design of efficient systems.

References

1. Ensminger D, Bond LJ (2011) Ultrasonics: fundamentals, technologies, and applications, 3rd edn. CRC Press, Boca Raton
2. Shchukin DG, Skorb E, Belova V, Möhwald H (2011) Ultrasonic cavitation at solid surfaces. Adv Mater 23(17):1922–1934
3. Marmottant P, Hilgenfeldt S (2003) Controlled vesicle deformation and lysis by single oscillating bubbles. Nature 423(6936):153–156
4. Shah YT, Pandit AB, Moholkar VS (1999) Cavitation reaction engineering. Kluwer Academic/Plenum Press, New York
5. Thompson LH, Doraiswamy LK (1999) Sonochemistry: science and engineering. Ind Eng Chem Res 38(4):1215–1249
6. Giacomello A, Chinappi M, Meloni S, Casciola CM (2013) Geometry as a catalyst: how vapor cavities nucleate from defects. Langmuir 29(48):14873–14884

7. Zhang L, Belova V, Wang HQ, Dong WF, Möhwald H (2014) Controlled cavitation at nano/microparticle surfaces. Chem Mater 26(7):2244–2248
8. Parkar PA, Choudhary HA, Moholkar VS (2012) Mechanistic and kinetic investigations in ultrasound assisted acid catalyzed biodiesel synthesis. Chem Eng J 187:248–260
9. Minnaert M (1933) On musical air bubbles and the sounds of running water. Philos Mag 16(104):235–248
10. Suslick KS (1990) Sonochemistry. Science 247(4949):1439–1445
11. Bang JH, Suslick KS (2010) Applications of ultrasound to the synthesis of nanostructured materials. Adv Mater 22(10):1039–1059
12. Gogate PR, Tayal RK, Pandit AB (2006) Cavitation: a technology on the horizon. Curr Sci 91(1):35–46
13. Flannigan DJ, Suslick KS (2005) Plasma formation and temperature measurement during single-bubble cavitation. Nature 434(7029):52–55
14. Suslick KS, Eddingsaas NC, Flannigan DJ, Hopkins SD, Xu H (2011) Extreme conditions during multibubble cavitation: sonoluminescence as a spectroscopic probe. Ultrason Sonochem 18(4):842–846
15. Ashokkumar M (2011) The characterization of acoustic cavitation bubbles—An overview. Ultrason Sonochem 18(4):864–872
16. Storey BD, Szeri AJ (2001) A reduced model of cavitation physics for use in sonochemistry. Proc R Soc Lond A 457(2011):1685–1700
17. Toegel R, Gompf B, Pecha R, Lohse D (2000) Does water vapor prevent upscaling sonoluminescence? Phys Rev Lett 85(15):3165–3168
18. Sivasankar T, Paunikar AW, Moholkar VS (2007) Mechanistic approach to enhancement of the yield of a sonochemical reaction. AlChE J 53(5):1132–1143
19. Storey BD, Szeri AJ (2000) Water vapour, sonoluminescence and sonochemistry. Proc R Soc Lond A 456(1999):1685–1709
20. Didenko YT, Suslick KS (2002) The energy efficiency of formation of photons, radicals and ions during single-bubble cavitation. Nature 418(6896):394–397
21. Ashokkumar M, Lee J, Kentish S, Grieser F (2007) Bubbles in an acoustic field: an overview. Ultrason Sonochem 14(4):470–475
22. Bremond N, Arora M, Dammer SM, Lohse D (2006) Interaction of cavitation bubbles on a wall. Phys Fluids 18(12):121505
23. Jiao JJ, He Y, Leong T, Kentish SE, Ashokkumar M, Manasseh R, Lee J (2013) Experimental and theoretical studies on the movements of two bubbles in an acoustic standing wave field. J Phys Chem B 117(41):12549–12555
24. Stricker L, Dollet B, Fernández Rivas D, Lohse D (2013) Interacting bubble clouds and their sonochemical production. J Acoust Soc Am 134(3):1854–1862
25. Hansson I, Mörch KA (1980) The dynamics of cavity clusters in ultrasonic (vibratory) cavitation erosion. J Appl Phys 51(9):4651–4658
26. Moholkar VS, Warmoeskerken MMCG (2003) Integrated approach to optimization of an ultrasonic processor. AlChE J 49(11):2918–2932
27. Avvaru B, Pandit AB (2009) Oscillating bubble concentration and its size distribution using acoustic emission spectra. Ultrason Sonochem 16(1):105–115
28. Moholkar VS, Warmoeskerken MMCG, Ohl CD, Prosperetti A (2004) Mechanism of mass-transfer enhancement in textiles by ultrasound. AlChE J 50(1):58–64
29. Xu HX, Glumac NG, Suslick KS (2010) Temperature inhomogeneity during multibubble sonoluminescence. Angew Chem Int Ed 49(6):1079–1082
30. Sutkar VS, Gogate PR (2009) Design aspects of sonochemical reactors: techniques for understanding cavitational activity distribution and effect of operating parameters. Chem Eng J 155(1–2):26–36
31. Moholkar VS, Sable SP, Pandit AB (2000) Mapping the cavitation intensity in an ultrasonic bath using the acoustic emission. AlChE J 46(4):684–694
32. Tuziuti T, Yasui K, Iida Y (2005) Spatial study on a multibubble system for sonochemistry by laser-light scattering. Ultrason Sonochem 12(1–2):73–77

33. Burdin F, Tsochatzidis NA, Guiraud P, Wilhelm AM, Delmas H (1999) Characterisation of the acoustic cavitation cloud by two laser techniques. Ultrason Sonochem 6(1–2):43–51
34. Tsochatzidis NA, Guiraud P, Wilhelm AM, Delmas H (2001) Determination of velocity, size and concentration of ultrasonic cavitation bubbles by the phase-Doppler technique. Chem Eng Sci 56(5):1831–1840
35. Kadkhodaee R, Povey MJW (2008) Ultrasonic inactivation of *Bacillus* α-amylase. I. Effect of gas content and emitting face of probe. Ultrason Sonochem 15(2):133–142
36. Bai LX, Xu WL, Deng JJ, Li C, Xu DL, Gao YD (2014) Generation and control of acoustic cavitation structure. Ultrason Sonochem 21(5):1696–1706
37. Gogate PR, Tatake PA, Kanthale PM, Pandit AB (2002) Mapping of sonochemical reactors: review, analysis, and experimental verification. AlChE J 48(7):1542–1560
38. Yin H, Qiao YZ, Cao H, Li ZP, Wan MX (2014) Cavitation mapping by sonochemiluminescence with less bubble displacement induced by acoustic radiation force in a 1.2 MHz HIFU. Ultrason Sonochem 21(2):559–565
39. Louisnard O (2012) A simple model of ultrasound propagation in a cavitating liquid. Part II: primary Bjerknes force and bubble structures. Ultrason Sonochem 19(1):66–76
40. Parlitz U, Mettin R, Luther S, Akhatov I, Voss M, Lauterborn W (1999) Spatio-temporal dynamics of acoustic cavitation bubble clouds. Philos Trans R Soc London, Ser A 357(1751):313–334
41. Bai LX, Ying CF, Li C, Deng JJ (2012) The structures and evolution of Smoker in an ultrasonic field. Ultrason Sonochem 19(4):762–766
42. Bai LX, Deng JJ, Li C, Xu DL, Xu WL (2014) Acoustic cavitation structures produced by artificial implants of nuclei. Ultrason Sonochem 21(1):121–128
43. Mettin R, Luther S, Ohl CD, Lauterborn W (1999) Acoustic cavitation structures and simulations by a particle model. Ultrason Sonochem 6(1–2):25–29
44. Legay M, Gondrexon N, Le Person S, Boldo P, Bontemps A (2011) Enhancement of heat transfer by ultrasound: review and recent advances. Int J Chem Eng 2011:17
45. Ohl CD, Kurz T, Geisler R, Lindau O, Lauterborn W (1999) Bubble dynamics, shock waves and sonoluminescence. Philos Trans R Soc London Ser A 357(1751):269–294
46. Kalva A, Sivasankar T, Moholkar VS (2009) Physical mechanism of ultrasound-assisted synthesis of biodiesel. Ind Eng Chem Res 48(1):534–544
47. Sutkar VS, Gogate PR, Csoka L (2010) Theoretical prediction of cavitational activity distribution in sonochemical reactors. Chem Eng J 158(2):290–295
48. Cucheval A, Chow RCY (2008) A study on the emulsification of oil by power ultrasound. Ultrason Sonochem 15(5):916–920
49. Sivasankar T, Moholkar VS (2008) Mechanistic features of the sonochemical degradation of organic pollutants. AlChE J 54(8):2206–2219
50. Suslick KS, Skrabalak SE (2008) Sonocatalysis. In: Ertl G, Knözinger H, Schüth F, Weitkamp J (eds) Handbook of heterogeneous catalysis, 2nd edn. Wiley-VCH Verlag GmbH & Co. KGaA, Weinheim, pp 2007–2017
51. Luo J, Fang Z, Smith RL Jr (2014) Ultrasound-enhanced conversion of biomass to biofuels. Prog Energy Combust Sci 41:56–93
52. Vichare NP, Senthilkumar P, Moholkar VS, Gogate PR, Pandit AB (2000) Energy analysis in acoustic cavitation. Ind Eng Chem Res 39(5):1480–1486
53. Rooze J, Rebrov EV, Schouten JC, Keurentjes JTF (2013) Dissolved gas and ultrasonic cavitation—A review. Ultrason Sonochem 20(1):1–11
54. Gogate PR, Sutkar VS, Pandit AB (2011) Sonochemical reactors: important design and scale up considerations with a special emphasis on heterogeneous systems. Chem Eng J 166(3):1066–1082
55. Tran KVB, Kimura T, Kondo T, Koda S (2014) Quantification of frequency dependence of mechanical effects induced by ultrasound. Ultrason Sonochem 21(2):716–721
56. Hua I, Hoffmann MR (1997) Optimization of ultrasonic irradiation as an advanced oxidation technology. Environ Sci Technol 31(8):2237–2243

57. Eddingsaas NC, Suslick KS (2007) Evidence for a plasma core during multibubble sonoluminescence in sulfuric acid. J Am Chem Soc 129(13):3838–3839
58. Oxley JD, Prozorov T, Suslick KS (2003) Sonochemistry and sonoluminescence of room-temperature ionic liquids. J Am Chem Soc 125(37):11138–11139
59. Bradley M, Ashokkumar M, Grieser F (2013) Multibubble sonoluminescence in ethylene glycol/water mixtures. J Phys Chem B 118(1):337–343
60. Liu LY, Yang Y, Liu PH, Tan W (2014) The influence of air content in water on ultrasonic cavitation field. Ultrason Sonochem 21(2):566–571
61. Bussemaker MJ, Xu F, Zhang DK (2013) Manipulation of ultrasonic effects on lignocellulose by varying the frequency, particle size, loading and stirring. Bioresour Technol 148:15–23
62. Rezania S, Ye ZL, Berson RE (2009) Enzymatic saccharification and viscosity of sawdust slurries following ultrasonic particle size reduction. Appl Biochem Biotechnol 153(1–3):103–115
63. Kuijpers MWA, van Eck D, Kemmere MF, Keurentjes JTF (2002) Cavitation-induced reactions in high-pressure carbon dioxide. Science 298(5600):1969–1971